Flow Structures in the Wake of a Pile-Supported Horizontal Axis Tidal Stream Turbine

Jisheng Zhang[a,b*,_], Xiangfeng Lin[a,b], Risheng Wang[c], Yakun Guo[d,*], Can Zhang[a,b], Yuquan Zhang[a,e]

[a] Key Laboratory of Coastal Disaster and Defence (Hohai University), Ministry of Education, China.
[b] College of Harbor Coastal and Offshore Engineering, Hohai University, Nanjing, China.
[c] College of Civil Engineering, Shandong Jiaotong University, Jinan, China
[d] Faculty of Engineering & Informatics, University of Bradford, UK
[e] College of Energy and Electrical Engineering, Hohai University, Nanjing, China
*Corresponding Authors: Jisheng Zhang, Yakun Guo
Email addresses: jszhang@hhu.edu.cn (Jisheng Zhang), y.guo16@bradford.ac.uk (Yakun Guo)

Abstract: This study presents the results from laboratory experiments to investigate the wake structure in the lee side of a scaled three-bladed horizontal axis tidal stream turbine with a mono-pile support structure. Experiments are conducted for a range of approaching flow velocity and installation height of rotor. Analysis of the results shows that bed shear stress increases with the increase of approaching velocity and decrease of installation height within 2D (D is the diameter of the rotor) downstream of the rotor. The flow filed within 2D downstream of the rotor is greatly influenced by the presence of nacelle and the mono-pile. Low stream-wise ow velocity and large turbulence intensity level is detected along the flume center right behind the nacelle and mono-pile from 1D to 2D downstream of the rotor. Stream-wise velocity at the blade tip height lower than the nacelle increases sharply from 1D to 2D and gradually grows afterwards. Correspondingly, the turbulence intensity decreases quickly from 1D to 2D and slowly afterwards. Large bed shear stress is measured from 1D to 2D, which is closely related to turbulence induced by the mono-pile. It is also found that the presence of the mono-pile might make the flow field more 'disc-shaped'.

Key Words: wake; turbulence structures; mono-pile; tidal stream turbine
PACS: 88.60K-, 88.60kc, 88.60.nh

1. Introduction:

There is a globally increasing demand for renewable energy in order to reduce the carbon dioxide emission due to the use of conventional fossil fuel. Tidal energy is one of the most promising renewable energy among all the alternatives for its predictability. Tidal cycles can be predicted in advance of time with a time-varying flow speed and direction, which is beneficial for controlling the electricity grid since the generation can be forecasted accurately [1]. Tidal stream turbines are normally preferable since they are usually installed in such a water depth that vessels can pass

above them, which allows to make full use of the channel. Compared with other types of renewable resources, such as wind energy [2] or wave energy [3,4], tidal stream energy is more stable and predictable. Furthermore, many sites where tidal turbines are placed as an array or a farm have strong tidal flows with a large peak flow speed [5, 6]. Considering the high density of sea water, large amount of energy can be extracted from these sites, making tidal turbines commercially viable.

As tidal flow passes tidal stream turbines, turbulent wake structures will be generated in the lee side of turbines. Such wake structure will affect the performance of tidal stream turbines. To fully understand the wake structures in the lee of a tidal stream turbine is as important as to characterize the power output of it. Turbines are normally arranged in farms and arrays to maximize the economical profit. Wake recovery length is of importance to determine inter-device spacing. For example, turbines spaced too close will suffer a decrease in performance; while turbines placed too far apart will result in a sub-optimal use of surface area within the region of strong tidal flow [7]. Furthermore, understanding the wake structure can help to investigate the potential effect of tidal turbines on the seabed scour [8, 9]. Due to its practical importance, extensive studies have been conducted to investigate the characteristics of the wake structure in the lee of a tidal turbine which is presented by an actuator disc.

Bahaj et al. [10] conducted experiments in a 21m long tilting flume. Both the wake structure and thrust exerted on the disc (tidal turbine) were measured. They found that the expansion of the wake was restricted by the free surface and sea bed. Based on this study, Myers and Bahaj [7] further investigated the wake structures when discs were placed in four different water depths. A significant increase in wake velocity deficit was observed when the disk was placed close to the bed. The turbulent kinetic energy (TKE) increased with the increase of the distance between the disk and bed. Such increase of TKE can aid mixing of the wake and free stream fluid and ultimately reduce the downstream wake velocity deficits. Although actuator discs are capable of simulating wake characteristics of a turbine to some extent, there are still flow features, such as swirl effects in the near wake, not captured well enough in this way. To overcome this, Myers and Bahaj [11] measured the wake of a 1/20th-scale horizontal axis turbine with an upright support structure. They found that the support structure increased the turbulence intensity (TI) level near to the free surface and the presence of a support structure would slightly slow down the wake recovery. Maganga et al. [12] investigated the impacts of TI using a tri-blade turbine model and a faster recovery of the flow was observed with a larger TI. This finding is also verified by Harrison et al. [13] who applied BEM-CFD method. Furthermore, when TI levels increase, the effects induced by the hub, turbine body and supporting structure is less noticeable because of the decrease of the velocity deficit and the non-development of the wake of the hub. Stallar et al. [14] investigated the wake structure downstream of a series of turbines in a flume. All turbines used were three bladed and had a diameter of 0.27m. They found that the velocity recovered to within 20% of the incident flow by x=10D. Beyond x=10D, recovery of mean velocity was slow. Tedds

et al. [15] measured the near wake characteristics of a turbine with a diameter of 0.5m in the high-speed recirculating water flume. They found that the free surface could result in asymmetric velocity distribution. The swirl induced by the turbine blade rotation was also observed and the magnitude of the span-wise velocity was all less than 10% of the stream-wise velocity. Highly anisotropic flow was observed downstream closest to the turbine while flow gradually became isotropic further downstream. Chen et al. [16] studied the development of the wake structure and found that wake rotation occurred immediately downstream. The circumfluence velocity was up to 20% of the stream-wise flow velocity. They also found that two wakes induced by turbine rotation and stanchion rapidly merged into a single wake, which led to the initial upwards movement of the wake.

These studies demonstrate that a rotating tidal stream turbine can significantly affect the wake structure. However, the effect of the mono-pile support structure on the wake structure has received less attention and is poorly understood. In previous studies, turbines were mainly replaced by an actuator disc or a rotor with an upright structure was used, while in this study, we focus on a horizontal tidal turbine which is placed with a mono-pile support structure. The existence of the mono pile can affect downstream flow characteristics, especially in the near wake. Good understanding of the wake structure is crucial to design sea bed protection and optimize tidal turbine layouts in an array. To this end, experiments are conducted in an open flume to investigate the wake structure of a three-bladed horizontal axis tidal stream turbine with a mono-pile support structure. The wake fields with various approaching velocities and installation heights are measured. It is expected that this study will enhance our understanding of wake structures of a tidal turbine affected by its support structure.

2. Experiments

2.1 Experimental Set-up

Experiments are carried out at the flume (see Fig.1), which is glass-sided with a working section 50 m in length, 1.2 m in width and 1.2 m in depth. At the upstream end of the working section, water is pumped into flume from a large chamber beneath the flume by centrifugal pumps. Pumped water flows through a honeycomb straightener to damp the rotational flow component induced in the inlet to generate a uniform flow. At the downstream end, water is returned into the chamber by pump to form a circulation system.

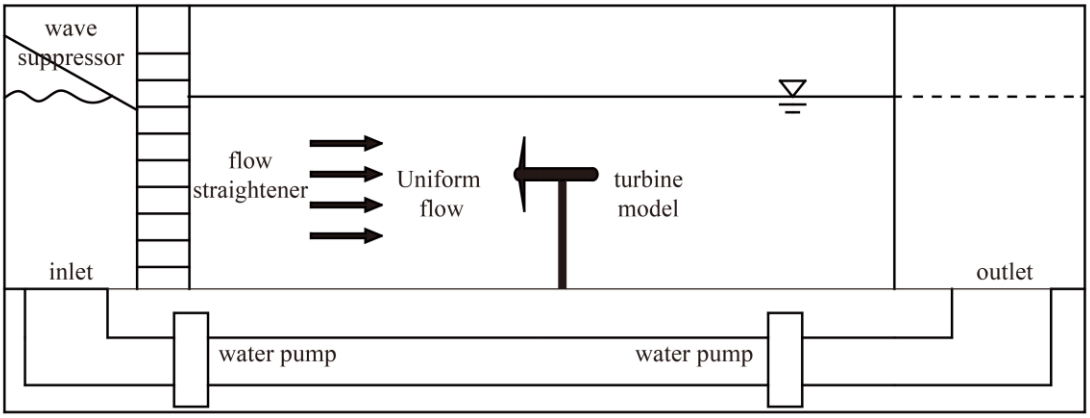

Fig.1 The schematic display of the flume used in this study

A stainless three-bladed model turbine is used in this study. The turbine consists of a rotor with a diameter of D=0.27 m, a nacelle with a diameter of 0.15D and a length of 0.8D, and a mono pile with a diameter of 0.1D. The rotor blade is designed with the NACA63-8xx type airfoil and subsequently optimized using the Blade Element Modelling Theory [17]. A small motor is placed inside the nacelle to provide a resistance torque against force imposed on blades by flow so that the rotor will not rotate in an unrealistic high speed. The mono pile is adjustable and thus, the installation height of the rotor, which is defined as the distance between the rotor hub center and the bottom of the flume, can be changed.

Water depth is maintained at 540 mm, two times of the rotor diameter, throughout the experiments. The turbine is placed 25 m away from the flow straightener so that the approaching flow is fully developed before reaching the model turbine.

2.2 Velocity Measurement

Flow field is measured using a downward-facing Nortek Vectrino Profiler (Nortek AS, Rud, Norway) which is capable of measuring three-dimensional velocities. The profiler used has a sample rate of 100Hz. As shown in Fig.2, little change can be observed when the duration for each measurement is more than 2 minutes. Therefore, 2 minutes is taken as the measurement duration for all measurements in this study. Throughout the experiment the signal to noise ration (SNR) is maintained above 15 by adding suspended particle into the flume. Similarly, the correlation of collected data is maintained higher than 70%. After collecting data, raw data are filtered to remove spikes (using the phase-space threshold method [18]) and those filtered data are replaced using an polynomial interpolation method.

In this study, 8 cases with various mean approaching velocity and installation heights are conducted (see Table 1). Flow Reynolds number and flow Froude number is calculated as $\mathrm{Re} = U_0 H/\nu$ and $\mathrm{Fr} = U_0/\sqrt{gH}$ respectively. In each case, one horizontal plane and one vertical plane, both cross the hub center of the turbine, are measured with the velocity profiler, as shown in Fig.3. For the horizontal plane, flow

field is measured on both sides of the rotor turbine, while for the vertical plane, flow field is measured from the channel bed to free water surface with every three centimeters interval. Data collected in these cases are post-processed to investigate wake characteristics of the three-bladed model turbine with a mono-pile support structure as well as to examine the effects of various installation heights and mean approaching flow velocities on wake structure.

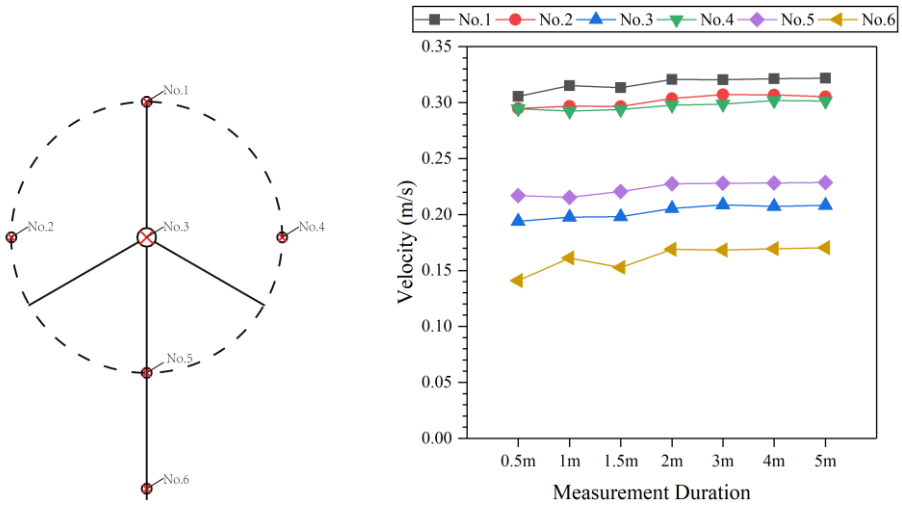

(a) (b)

Figure 2: Validation of measurement duration sensitivity. (a) shows measured points for duration sensitivity, in which all points are located at x = 1D, and No.6 is 1cm above the flume bottom.

Table 1 Experimental cases

No.	Mean Approaching Velocity (m/s)	Installation Height (m)	Re.	Fr.
1	0.35	0.8D	192500	0.151
2	0.35	0.9D	192500	0.151
3	0.35	1.0D	192500	0.151
4	0.35	1.1D	192500	0.151
5	0.35	1.2D	192500	0.151
6	0.3	1.0D	165000	0.129
7	0.4	1.0D	220000	0.172
8	0.45	1.0D	247500	0.192

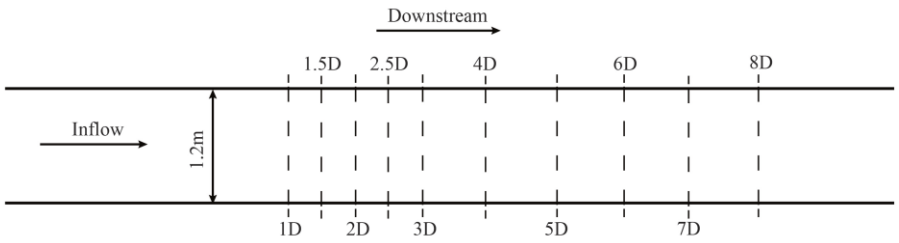

(a) Locations of cross-sections where velocity was measured, the turbine rotor plane was located at x = 0D

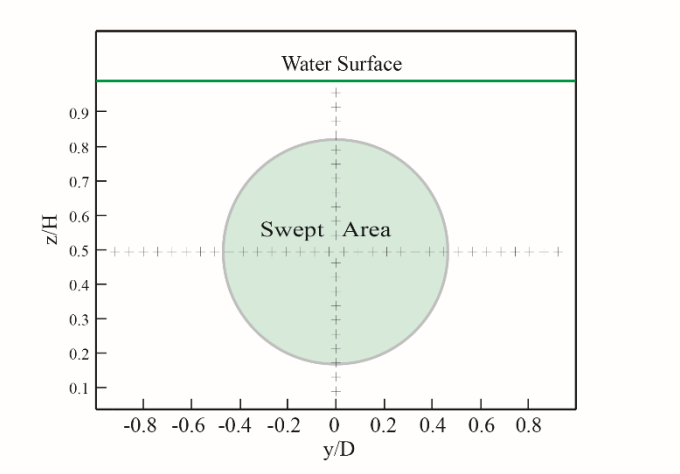

(b) Locations of velocity measurement at all cross-sections

Fig.3 Velocity measurement locations

2.3 Turbulence Intensity

The dimensionless TI and TKE can be calculated as [10, 11]:

$$\mathrm{TI} = \frac{\sqrt{\frac{1}{3}(u'^2 + v'^2 + w'^2)}}{U_0} \qquad (1)$$

$$TKE = \frac{1}{2}(u'^2 + v'^2 + w'^2) \qquad (2)$$

where u', v', w' are fluctuating velocity in x, y, z direction, respectively and can be calculated as:

$$u' = \sqrt{\frac{1}{N}\sum_{i=1}^{N}(u_i - \bar{u})^2} \qquad (3)$$

$$v' = \sqrt{\frac{1}{N}\sum_{i=1}^{N}(v_i - \bar{v})^2} \qquad (4)$$

$$w' = \sqrt{\frac{1}{N}\sum_{i=1}^{N}(w_i - \bar{w})^2} \qquad (5)$$

2.4 Turbulence Anisotropy

To investigate the anisotropy of the turbulent flow field in the lee side of the turbine, the non-dimensional anisotropic part of the Reynolds stress tensor or simply anisotropy tensor b_{ij} is used (Choi and Lumley [15]):

$$b_{ij} = \begin{pmatrix} \frac{u'^2}{2TKE} - \frac{1}{3} & \frac{u'v'}{2TKE} & \frac{u'w'}{2TKE} \\ \frac{u'v'}{2TKE} & \frac{v'^2}{2TKE} - \frac{1}{3} & \frac{w'v'}{2TKE} \\ \frac{u'w'}{2TKE} & \frac{w'v'}{2TKE} & \frac{w'^2}{2TKE} - \frac{1}{3} \end{pmatrix} \quad (6)$$

The invariants I, II, III which are used to characterize turbulence anisotropy are defined as following:

$$I = b_{kk}$$
$$II = -b_{ij}\, b_{ji}/2$$
$$III = b_{ij} b_{jk}\, b_{ki}/3$$

To simplify the anisotropy tensor, another two invariants, η and ξ are introduced:

$$\xi^3 = III/2, \eta^2 = -II/3$$

As it is stated in Lumley [16], the case of $\xi = \eta = 0$ corresponds to isotropic turbulence. When $\xi > 0$, a single diagonal component of the anisotropy tensor dominates over the other two components and the shape of the tensor is 'rod-liked'. When ξ<0, two equal diagonal components of the anisotropy tensor dominate over the third smaller diagonal component, and the shape of the tensor is 'disc-shaped'.

2.5 Bed Shear Stress

Considering complexity of the flow field in the wake of the model turbine, the TKE method is employed to calculate local bed shear stress in this study. As suggested by Biron et al. [17], the TKE approach seems to be one of the most appropriate methods in a complex flow field. Using the TKE method, bed shear stress τ_0 is defined as:

$$\tau_0 = C_1 \rho TKE$$

where C_1 is a proportionality constant, taken as 0.19 [18].

Biron et al. [17] suggested that positioning the instrument at 10% of the flow depth is probably the best option when using single point measurements as this position is likely to be less affected by unexpected increases in SNR that may occur near the bed. Therefore, the measured points for estimating bed shear stress are set at 50 mm above the flume bottom in this study.

3. Results and Discussion

3.1 Wake Velocity Distribution

Fig.3.a-c shows velocities in three directions measured from x=1D to 8D in the horizontal plane for Case 3. It can be seen from Fig.3.a that the largest velocity deficit is located at x=1D, which is immediately behind the nacelle. The stream-wise velocity is around $0.5U_0$ at x=1D. This is slightly different from the observation of Tedds et al. [11] who found that the largest velocity deficit was behind the tip of blades. This difference is maybe due to the fact that the rotor in this study rotated in a rather lower speed than that in Tedds et al. [11]. As such, the resultant effect of the rotor rotation on flow field in this study is insignificant. Due to the blockage of the model turbine,

flow at both sides of the flume is accelerated. As water flows downstream, it gains energy from ambient flow and flow velocity increases gradually. Large increase of flow velocity is seen from x=1D to 2D and downstream of x=2D, only small increase of flow velocity is observed.

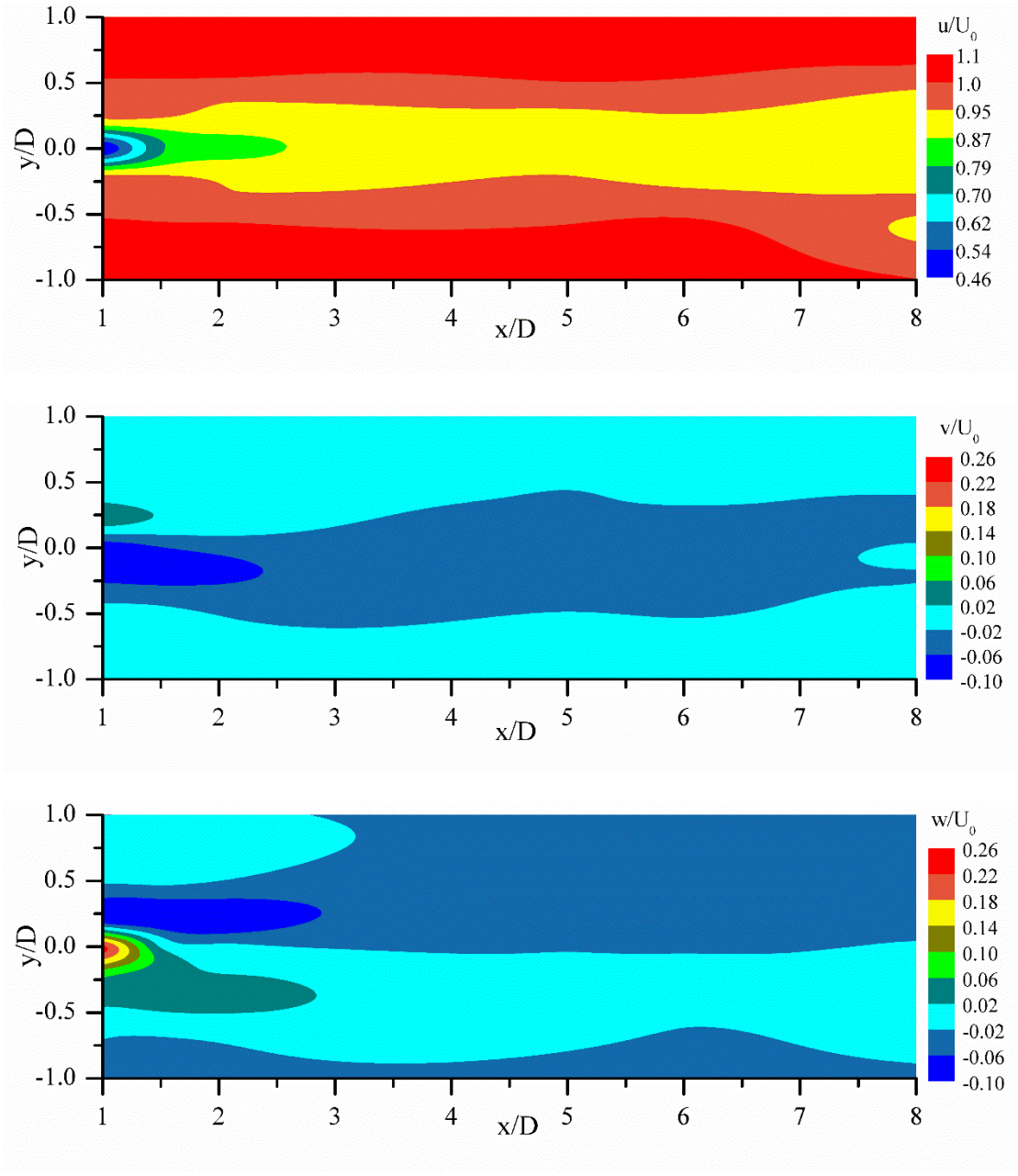

Fig.3 Measured velocities in the horizontal plane for Case 3: a) u, stream-wise velocity; b) v, transverse velocity; c) w, vertical velocity

Fig.3b-c shows that the transverse and vertical velocity components dissipate quickly from x=1D to 2.5D and downstream of x=2.5D, they become negligible. Reverse transverse and vertical velocities are seen to occur on either sides of the flume within x=2.5D, indicating the swirl structure generated due to the rotor's rotation. At y=0D and x=1D, flow velocity with a vertical component up to $0.26U_0$ and a transverse component up to $0.1U_0$ is observed. Flow structure is affected by the

vortex shedding from the nacelle as well as the rotor rotation and is very complicated.

Stream-wise velocity component in the vertical plane for Case 3 is presented in Fig.4.a-c. Several factors, such as the rotor rotation, the existence of the rotor nacelle and the support structure affect velocity in the downstream field of a tidal stream turbine.

In Fig.4, the largest velocity deficit is observed at the height of the rotor nacelle, around z=0.5H, along the flume. From x=1D to 8D at this height, the velocity recovers approximately from $0.5U_0$ to $0.85U_0$ with the rapid recovery taking place from 1D to 2D. This is consistent with previous studies [11, 12], where flow recovery rate is lager in the near wake and much smaller after the near wake.

Significant velocity deficit is also observed at the height of blade tips both above and beneath the rotor hub, especially within x=2D. Above the rotor hub at around $z = 0.73H$, flow velocity increases from $0.79U_0$ in x=0.5D to $0.98U_0$ in x=2D. Flow velocity almost remains the same downstream of x=2D. Flow velocity recovery beneath the rotor hub at around $z = 0.25H$ has a similar trend, except that after x=2D, the flow continues to speed up and reaches around $0.8U_0$ at x=8D.

The effect of the mono pile on flow structure is evaluated by comparing flow velocities above and beneath the rotor hub. Larger velocity deficit beneath the rotor hub can be observed especially from x=1D to 2D. Downstream of x=2D, only slight increases in flow velocity is observed above the rotor hub, while beneath the rotor hub, obvious flow recovery can be still seen to occur.

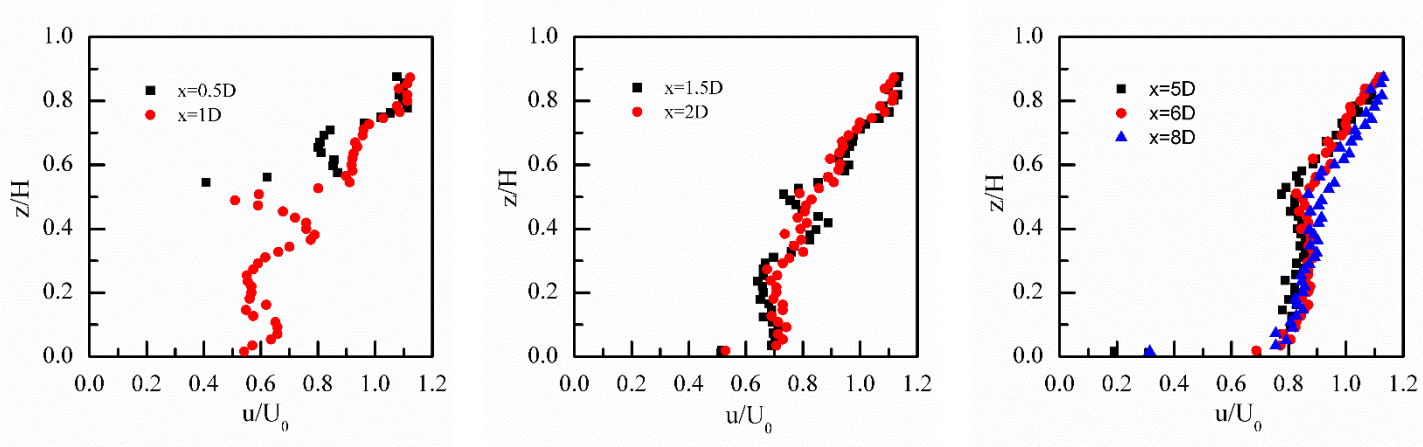

Fig.4 Stream-wise velocity component in the vertical plane downstream of the model tidal stream turbine

Fig. 5a-c is the transverse velocity component, showing a similar trend of velocity distribution at various downstream distances of the model tidal stream turbine. Corresponding to the anticlockwise rotation of the rotor blade, transverse velocity above the central line is negative and gradually increases from top to the nacelle. Downwards, velocity tends to be positive and reaches the largest value at around $z = 0.4H$. As water flows downstream, influence of rotor ration is alleviated. At x=1D, both the maximum positive value and negative value reaches $0.14U_0$. However, At x=8D, the maximum negative value increases to $0.7U_0$ and the maximum positive value is close to zero, which indicates that the swirl induced by the rotor rotation tends to vanish in further downstream. Measured vertical velocity in the

vertical plane is very small in this study.

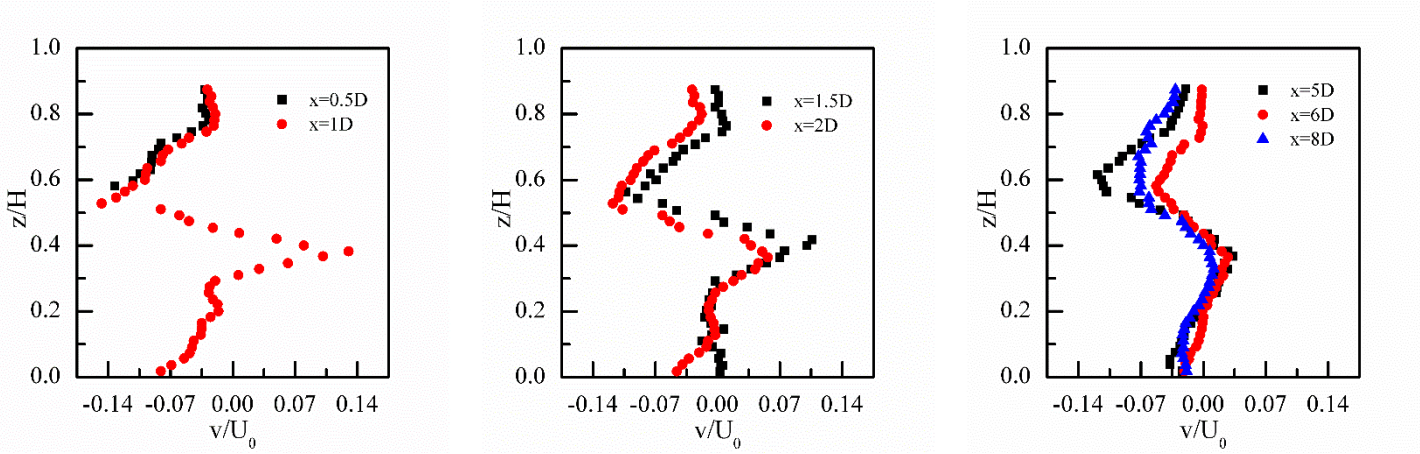

Fig.5 Transverse velocity component in the vertical plane downstream of the model tidal stream turbine

3.2 Turbulence Structures

3.2.1 Turbulence Intensity

Fig.6 show the dimensionless TI distribution in the horizontal plane downstream of the three-bladed turbine. Within x=3D, the largest value of TI is found along the central line (y=0D). A value up to 17% is found right behind the nacelle, which has a close relationship with vortices shedding from the nacelle. At the central line, the TI decreases from 17% at x=1D to around 8% at x=3D. At locations being larger than 3D (x>3D), TI maintains almost at this level and only slight decrease is observed. Two small peaks of the TI are observed at the blade tips ($y = \pm 0.5D$) at x=1D, indicating that vortices induced by the rotor rotation can also affect the turbulence in the wake. Compared with turbulence caused by the rotor rotation and that caused by flow passing the nacelle, it is found that within x=3D, the presence of the nacelle has a larger influence than the rotor rotation.

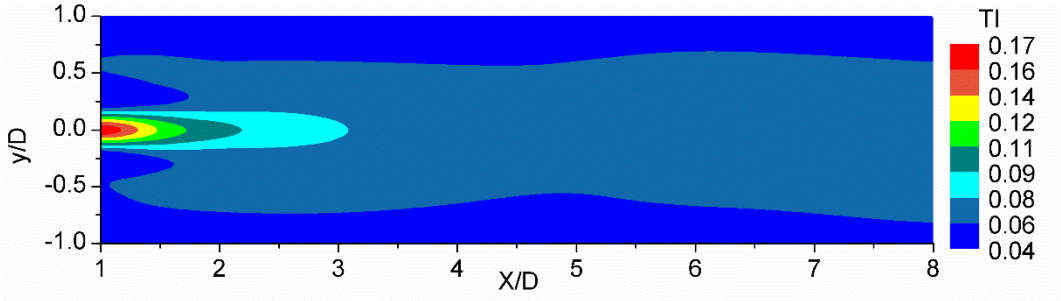

Fig.6 Turbulent intensity (TI) in the horizontal plane downstream of the model tidal stream turbine

Distributions of TI in the central vertical plane are presented in Fig.7.a-c. A small peak is observed around the blade tip ($z = 0.74H$) up to x=8D. At this height, TI maintains around 7.5% throughout the measured area. A large value of TI is found in the area beneath the rotor hub. Compared with TI values above the rotor hub, the peak value for various distances downstream beneath the rotor hub is larger, especially within x=2D. However, the peak value decreases quickly, from 25% in x=1D to 15% in x=2D. The higher value of TI beneath the rotor hub may have a close relationship with highly turbulent and complex flow structures after flow passes the

mono pile. However, the effect induced by the mono pile tends to be alleviated downstream of x=5D as it can be seen in Fig.7.c that TI along the vertical line from the top to the bottom almost maintains as 7.5% and no obvious peak values are observed beneath the rotor hub.

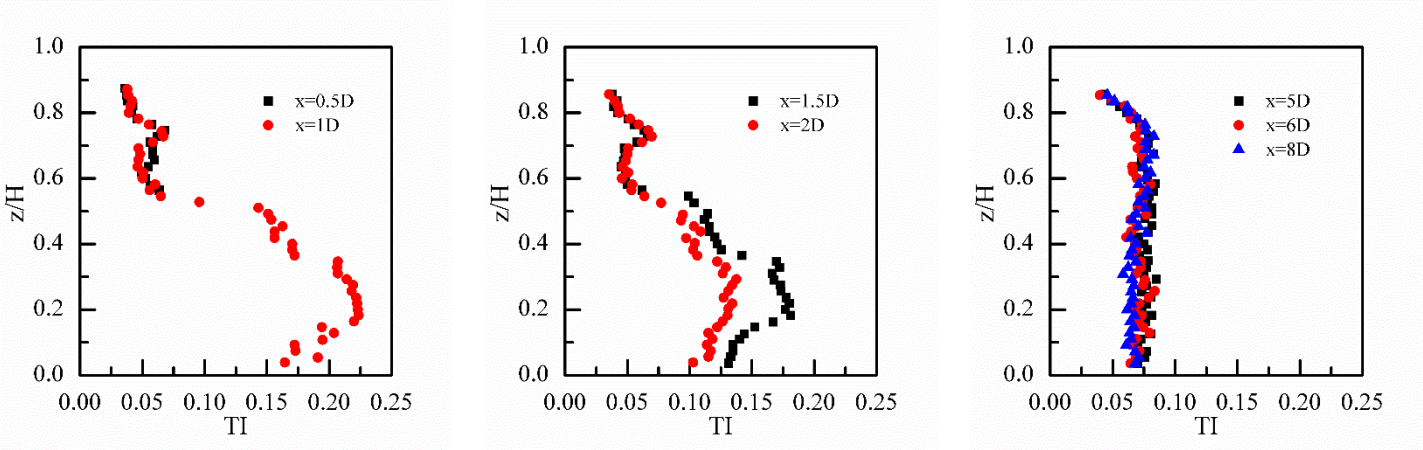

Fig.7 Turbulence intensity (TI) in the vertical plane downstream of the model tidal stream turbine

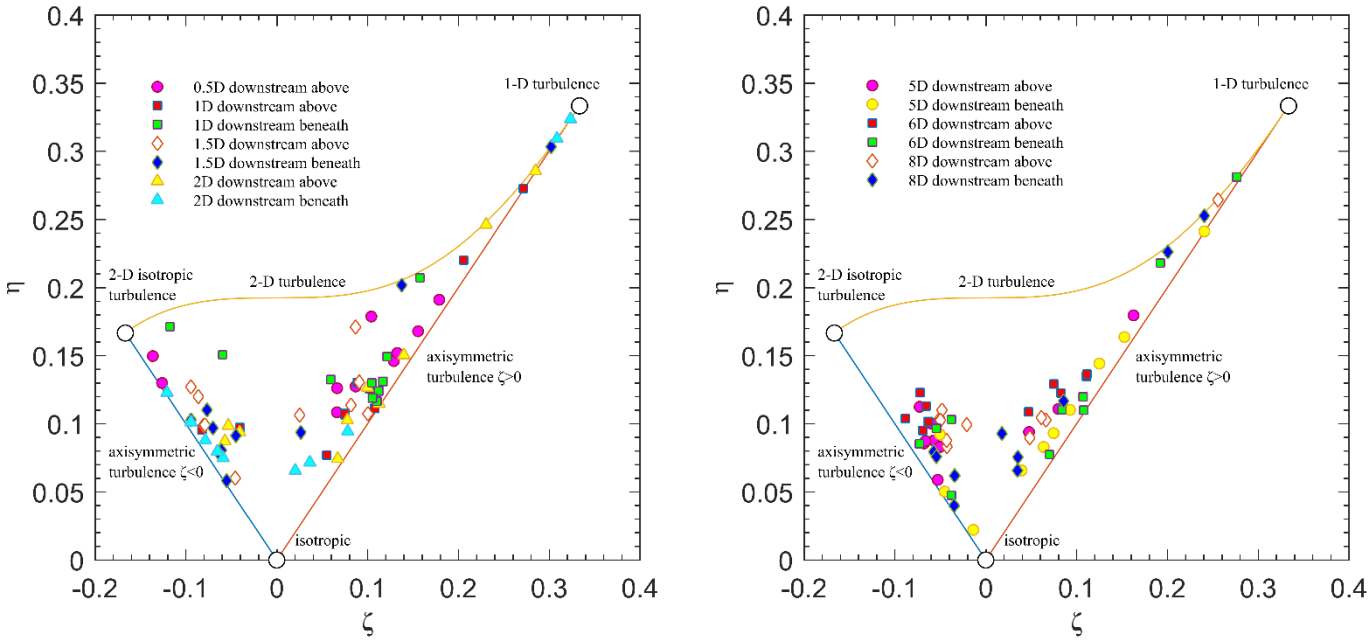

Fig.8 Lumley triangles showing the turbulence anisotropy downstream of the turbine

3.2.2 Turbulence anisotropy

Fig. 8 is the anisotropy tensor data, showing the comparison of the turbulence anisotropy of flow filed above and beneath the rotor hub height for evaluating the effect of the mono-pile structure on turbulence structure downstream of the turbine. Fig.8.a shows the downstream data closest to the turbine, and there are larger ξ and η values. This means that the flow is highly anisotropic. Although in the far wake region, the flow gradually becomes more isotropic as expected, the turbulence is still strongly anisotropic in x=8D, indicating that the presence of turbine still applies effect

on the flow structure. Fig. 8 also shows that the presence of mono pile further increases downstream turbulence anisotropy. These data show that due to the presence of the support structure, the flow tends to be more 'rod-shaped' and further downstream, this effect is gradually mitigated.

3.3 Effects of approaching velocity

Fig.9 shows bed shear stress downstream of the model turbine with various mean approaching velocities. It is seen that the bed shear stress decreases with the increase of downstream distance away from turbine with sharp decrease taking place from x=1D to x=2D. Fig. 9 also shows that the larger incoming flow velocity generates greater bed shear stress.

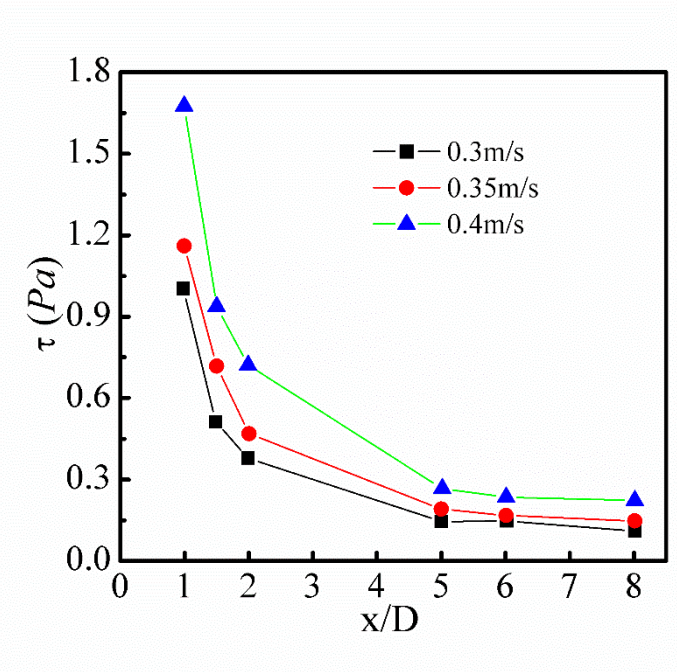

Fig.9 Bed shear stress with various approaching mean velocities

Fig. 10a-f shows the normalized stream-wise velocity (U/U_0, U_0 is the mean incoming velocity) and dimensionless TI along the central line at the blade tip height above the rotor hub (Fig. 10a-b); at the rotor hub height (Fig. 10c-d) and at the blade tip height beneath the rotor hub (Fig. 10e-f). Fig10.a-b shows that the normalized velocity at the blade tip height above the rotor hub slightly increases with the increase of x while the TI has a low value and slightly decreases with x.

It can be seen from Fig.10.c-d that flow velocity at the rotor hub height increases sharply within x=2D while a gradual increase is seen downstream of x=2D. Larger incoming velocity generates relatively higher normalized velocity at the rotor hub height. As suggested by Mycek et al. [19], the flow recovery in the wake of a horizontal turbine is closely related to its turbulence intensity level. The sharp decrease of TI corresponds to the quickly increase of flow velocity from x=1D to 2D. Gradual decrease of TI is also observed downstream of x=2D. It is also seen that along the central line, the approaching velocity has insignificant effect on

dimensionless TI for x>5D.

The situation at the blade tip height beneath the hub rotor, shown in Fig10.e-f, demonstrates different trend. It is seen that the normalized velocity at this height increases with the increase of x though a rather sharp increase of velocity occurring within x=2D. the approaching mean velocity has great effect on TI which decreases with the increase of incoming velocity. comparing with the TI at other height, the TI at this height is much larger than those at other two heights. This may be due to the effect of the supported structure [7].

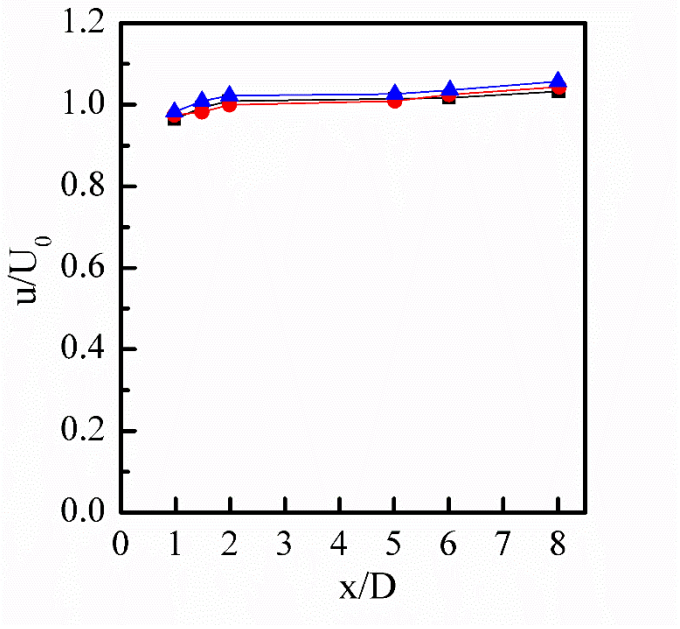

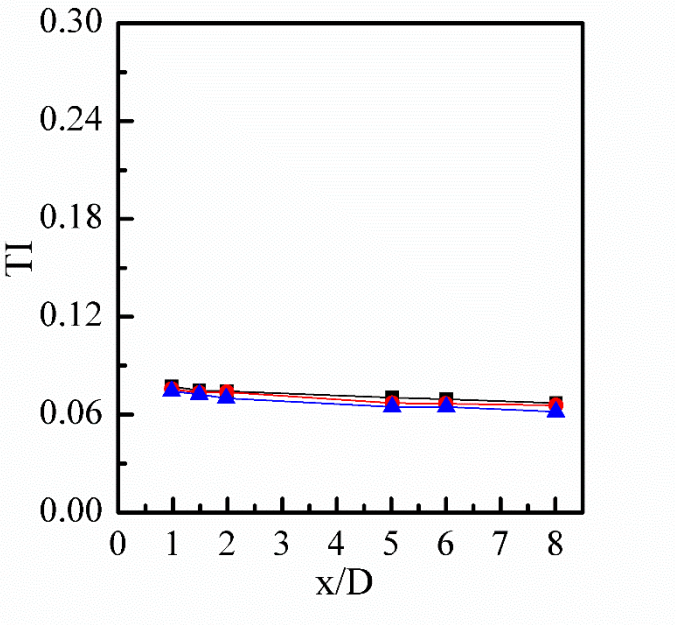

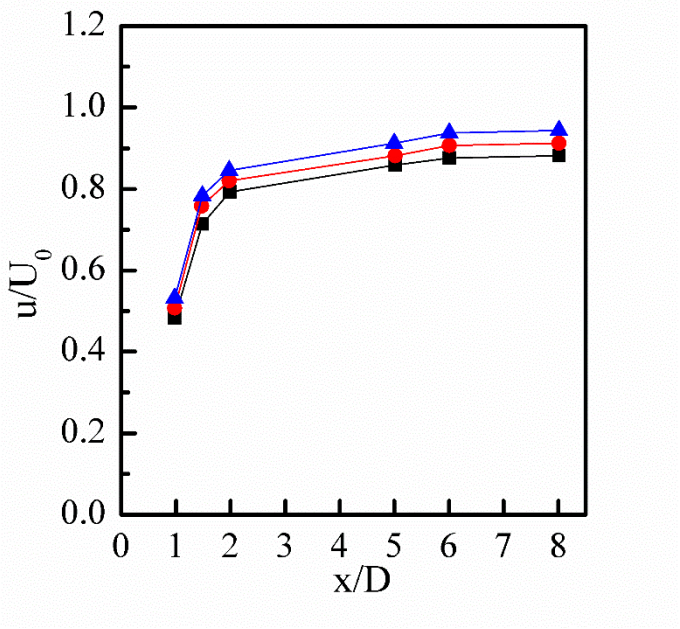

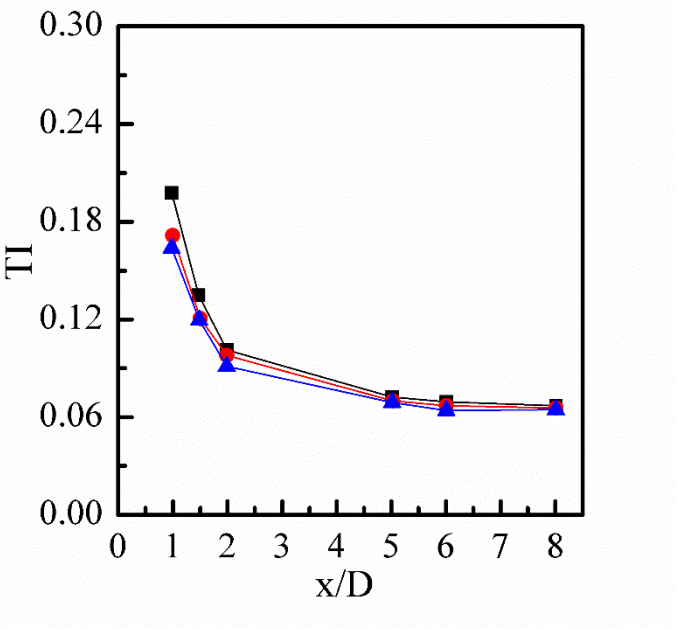

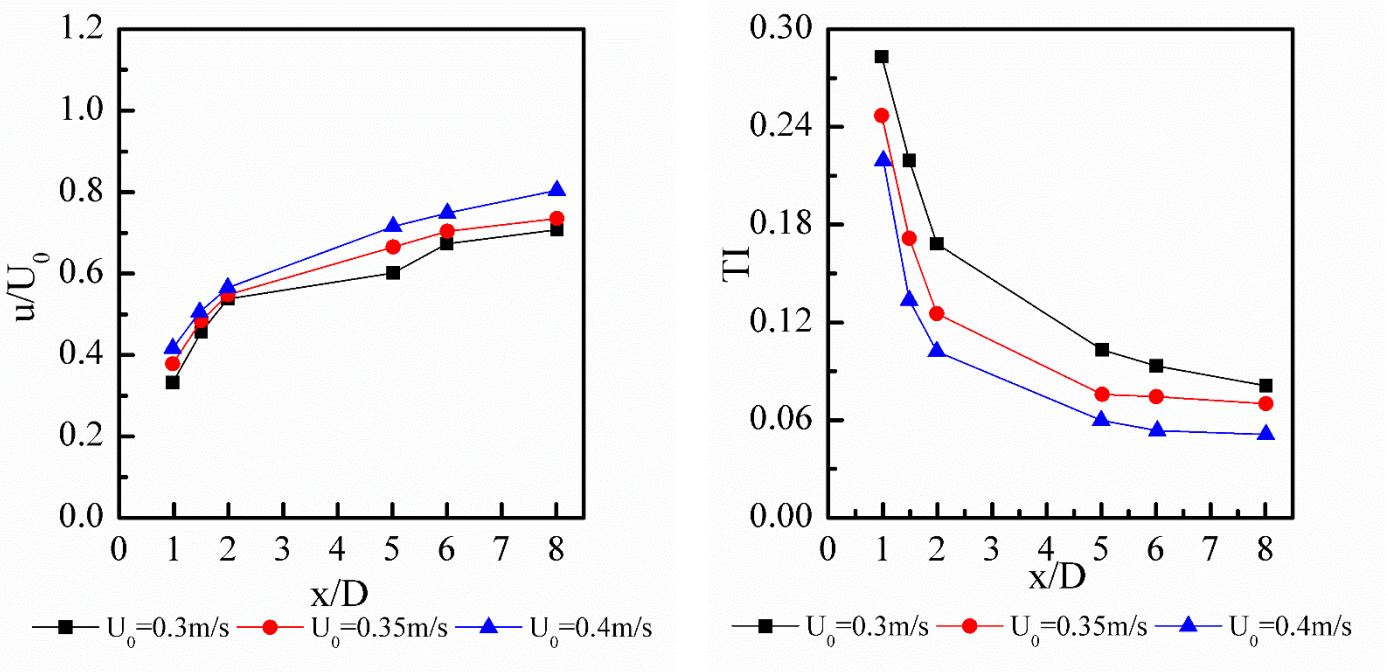

Fig.10 Flow characteristics along the central line with various mean approaching velocities: a-b: at the blade tip height above the rotor hub; c-d: at the rotor hub height; e-f: at the blade tip height beneath the rotor hub

3.4 Effects of installation height

The bed shear stress in the wake of the model turbine with various installation heights is shown in Fig.11, which shows that the installation height has insignificant effect of the bed shear stress. A sharp decrease of the bed shear stress is seen to occur within x=2D followed by a gradual decrease of the bed shear stress for x>2D.

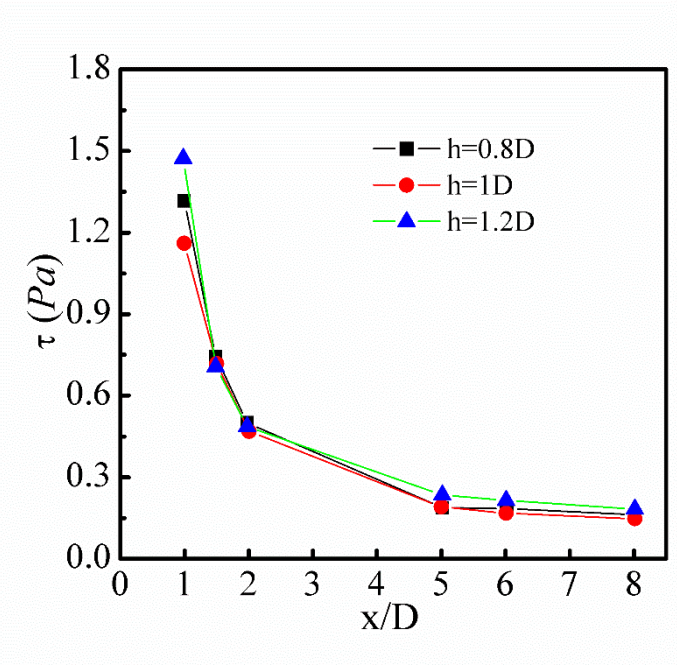

Fig.11 Bed shear stress with various installation heights

Fig.12.a-f is the normalized velocity and dimensionless TI at different heights with various installation heights while U_0 is maintained as 0.35m/s. Fig. 12 a shows

that the turbine installation height has negligible effect on the flow velocity recovery at the blade tip height above the rotor hub. At the rotor hub height (Fig.12.c) and at the blade tip height beneath the rotor hub (Fig. 12 e), flow velocity increases with the increase of the installation height, particularly for the flow velocity at the blade tip height beneath the rotor hub. The lower flow recovery for lower installation height may be closely related to the undisturbed distribution of the mean approaching velocity.

Fig.12.b shows that the installation height has insignificant effect on the TI along the central line at the blade tip height above the rotor hub. However, at the rotor hub height (Fig. 12d) and at the blade tip height beneath the rotor hub (Fig. 12 f), the dimensionless TI decreases with the increase of the installation height as well as with the increase of x. This may be related to turbulence generated by the flume bottom. Fig. 12b,d,and f also shows that the TI at the blade tip height beneath the rotor hub is much larger than those at other two heights.

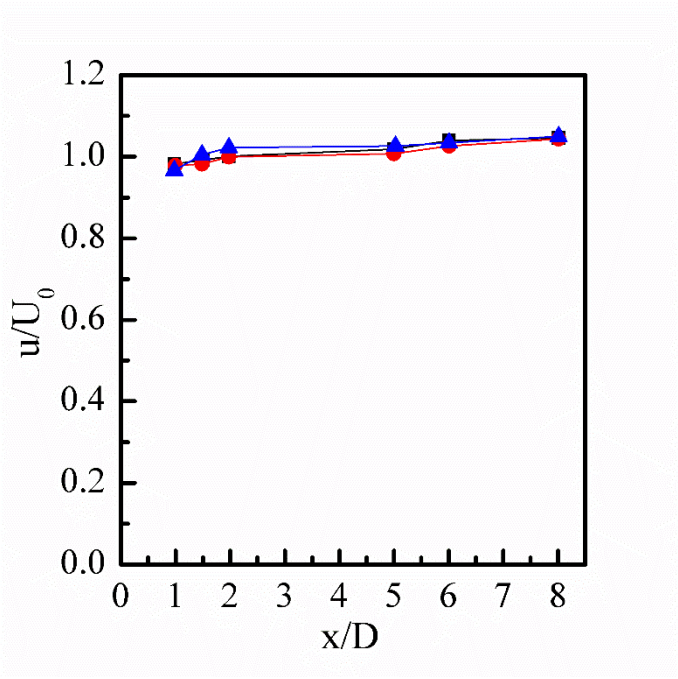

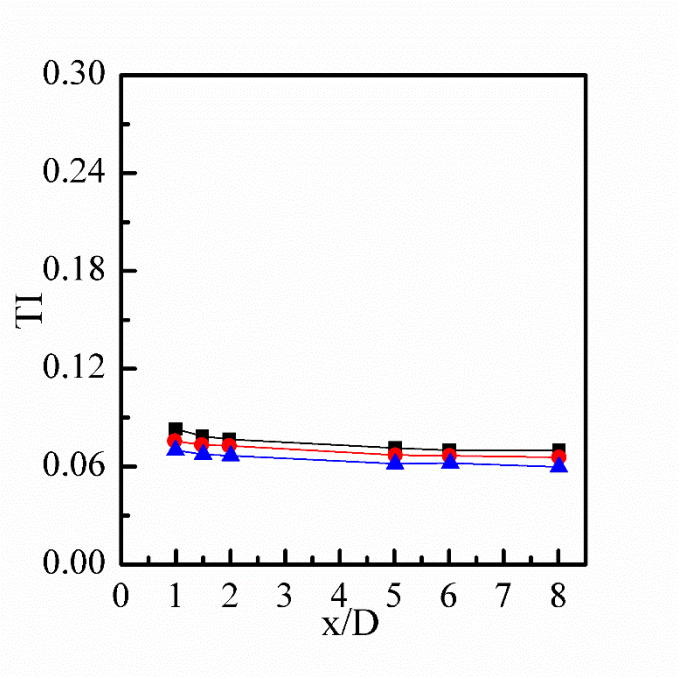

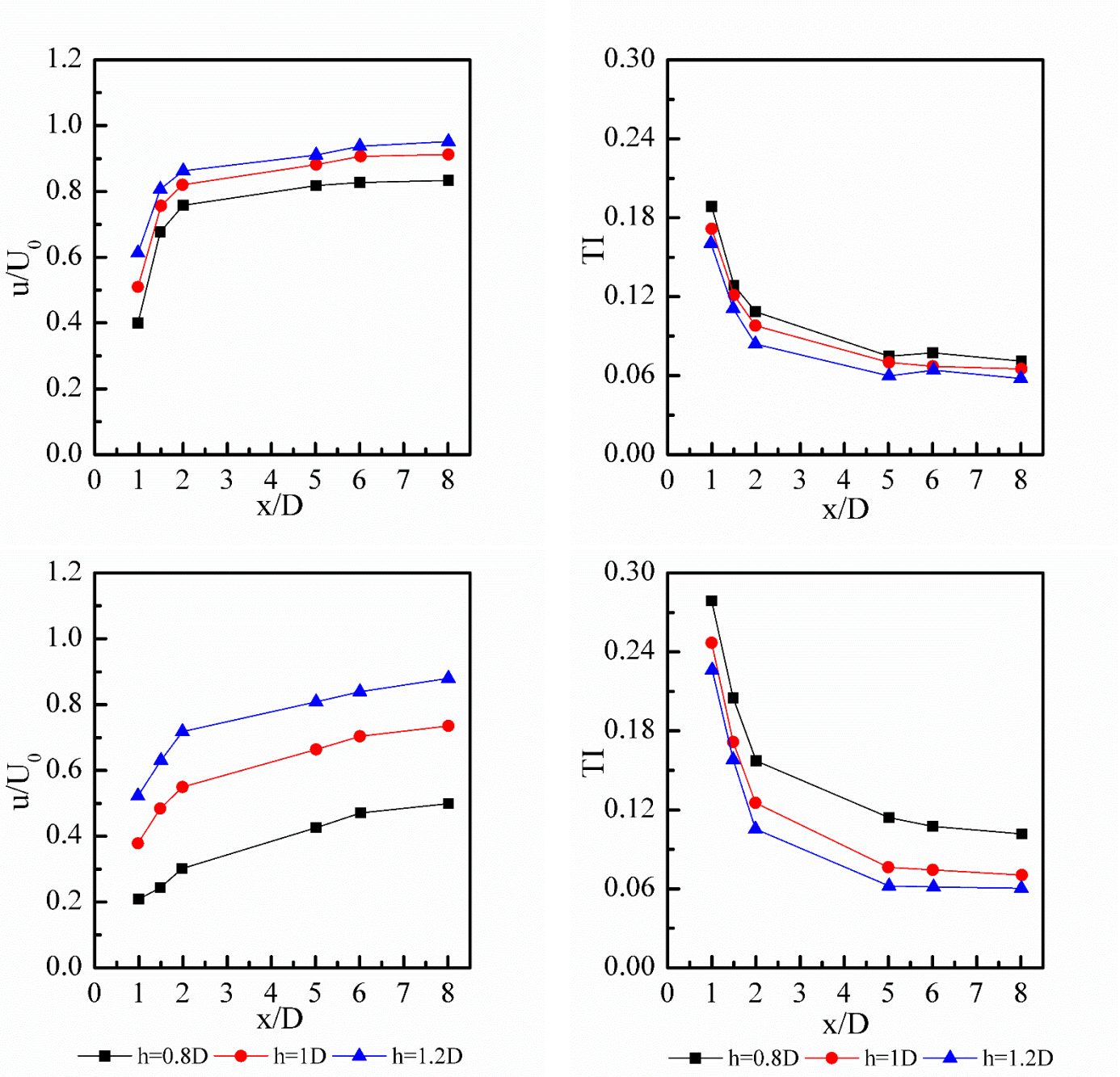

Fig.13 Flow characteristics along the central line with various installation heights: a-b: at the blade tip height above the rotor hub; c-d: at the rotor hub height; e-f: at the blade tip height beneath the rotor hub.

4. Conclusions

Experiments were conducted to further understand the downstream flow filed of a scaled horizontal tidal stream turbine with a nacelle and a mono-pile support structure. A full understanding of downstream flow filed of the tidal stream turbine is significant to optimize the layout of a tidal stream turbine farm and evaluate sea bed response to an operating turbine. Detailed ADV measurements were undertaken at a horizontal plane and a vertical plane across the turbine's rotor center to investigate three dimensional characteristics of downstream filed. The flow velocity distribution

was obtained and turbulence intensity was evaluated.

From x=1D to 2D, flow velocity and TI are both influenced greatly by the rotor rotation and structures. In the horizontal plane, the maximum velocity deficit and the largest TI was located at immediate behind the nacelle. The circumfluence velocity was up to $0.26U_0$. In the vertical plane, large velocity deficit was observed behind the mono pile and so was highly turbulent flow, which is due to the block of the support structure and vortices shed from it. It's also found that the existence of the mono pile intensifies the anisotropy of the downstream flow filed, making the flow turbulence more 'rod-shaped'. However, the effect of the rotor rotation and block of structures mitigates quickly from x=1D to 2D and after x=5D, only slight increases in the flow stream-wise velocity and turbulence level can be seen, while the circumfluence velocity tends to be negligible.

Impacts of the approaching velocity and installation height were also discussed in this study. It indicates that a larger approaching velocity may increase the bed shear stress downstream of the tidal stream turbine greatly and slightly increase the flow recovery rate. When turbines are installed at various heights, it sees that flow recovers much more quickly with a higher installation height at the rotor hub height and blade tip height above the rotor hub.

This study experimentally investigates downstream flow field characteristics of a tidal stream turbine with a nacelle and a mono-pile support structure, which is more realistic compared with previous researches, considering the way current commercially employed tidal stream turbines are installed in reality. Furthermore, effects of approaching velocities and installation heights on the downstream stream flow filed are also discussed.

Acknowledgements

This study was funded by Postgraduate Research & Practice Innovation Program of Jiangsu Province (KYCX17_0448).

References

[1] Clarke JA, Connor G, Grant AD, Johnstone CM. 2006. Regulating the output characteristics of tidal current power stations to facilitate better base load matching over the lunar cycle. Renewable Energy. 31(2), 173–180.

[2] Blunden L, Bahaj AS. 2007. Tidal energy resource assessment for tidal stream generators. Proceedings of the Institution of Mechanical Engineers, Part A: Journal of Power and Energy 221 (2), 137–146.

[3] Myers LE, Bahaj AS. 2005. Simulated electrical power potential harnessed by marine current turbine arrays in the Alderney Race. Renewable Energy. 30 (11), 1713–1731.

[4] Myers LE, Bahaj AS. 2010. Experimental analysis of the flow field around horizontal axis tidal turbines by use of scale mesh disk rotor simulators. Ocean Engineering. 37(2-3), 218-227.

[5] Chen L, Lam WH. 2014. Methods for predicting seabed scour around marine current turbine. Renewable and Sustainable Energy Reviews. 29, 683-692.

[6] Bahaj AS, Myers LE, Thomson MD, Jorge N. 2007. Characterising the wake of horizontal axis marine current turbines. Proceedings of the 7th European Wave and Tidal Energy Conference.

[7] Myers LE, Bahaj AS. 2009. Near wake properties of horizontal axis marine current turbines. Proceedings of the 8th European Wave and Tidal Energy Conference.

[8] Maganga F, Germain G, King J, Pinon G, Rivoalen E. 2010. Experimental characterization of flow effects on marine current turbine behavior and on its wake properties. IET Renew. Power Gener. 4 (6), 498-509.

[9] Harrison ME, Batten MJ, Bahaj AS. 2010. A Blade element actuator disc approach applied to tidal stream turbines. OCEANS 2010 MTS/IEEE SEATTLE. 1-8.

[10] Stallard T, Collings R, Feng T, Whelan J, 2013. Interactions between tidal turbine wakes: experimental study of a group of three-bladed rotors. Philos Trans Royal Soc. 371: 20120159.

[11] Tedds SC, Owen I, Poole RJ, 2014. Near-wake characteristics of a model horizontal axis tidal stream turbine. Renewable Energy. 63, 222-235.

[12] Chen YL, Lin BL, Lin J, Shujie Wang SJ, 2017. Experimental study of wake structure behind a horizontal axis tidal stream turbine. Applied Energy. 196, 82-96.

[13] Bavanish B, Thyagarajan K. 2014. Optimization of power coefficient on a horizontal axis wind turbine using bem theory. Renewable and Sustainable Energy Reviews. 26, 169-182.

[14] Goring DG, Nikora VI. 2002. Despiking Acoustic Doppler Velocimeter data. J. Hydraul, Eng. 128(1), 117-126.

[15] Choi KS, Lumley JL. 2001. The return to isotropy of homogeneous turbulence. J. Fluid Mech. 436, 59-84.

[16] Lumley JL, 1979. Computational modelling of turbulent flows. Advances in Applied Mechanics. 18, 123-176.

[17] Biron PM, Nobson C, Lapointe MF, Gaskin SJ, 2004. Comparing different methods of bed shear stress estimates in simple and complex flow fields. Earth Surf. Processes Landforms, 29,

1403-1415.

[18] Kim SC, Friedrichs CT, Maa PY, Wright LD, 2000. Estimating bottom stress in tidal boundary layer from Acoustic Doppler Velocimeter data. Journal of Hydraulic Engineering. 126, 399-406.

[19] Mycek P, Gaurier B, Germainb G, Pinona G, Rivoalena E, 2013. Numerical and experimental study of the interaction between two marine current turbines. International Journal of Marine Energy. 1, 70-83